Eur. Phys. J. Plus (2020) 135:546
https://doi.org/10.1140/epjp/s13360-020-00544-z

THE EUROPEAN PHYSICAL JOURNAL PLUS

Regular Article

Transverse dynamics of vector solitons in defocusing nonlocal media

G. N. Koutsokostas[1], **T. P. Horikis**[2,a], **D. J. Frantzeskakis**[2], **B. Prinari**[3], **G. Biondini**[3]

[1] Department of Physics, National and Kapodistrian University of Athens, Panepistimiopolis, Zografos, 15784 Athens, Greece
[2] Department of Mathematics, University of Ioannina, 45110 Ioannina, Greece
[3] Department of Mathematics, State University of New York at Buffalo, Buffalo, NY 14260, USA

Received: 17 March 2020 / Accepted: 17 June 2020

Abstract The transverse instability of line solitons of a multicomponent nonlocal defocusing nonlinear Schrödinger (NLS) system is utilized to construct lump and vortex-like structures in 2D nonlocal media, such as nematic liquid crystals. These line solitons are found by means of a perturbation expansion technique, which reduces the nonintegrable vector NLS model to a completely integrable scalar one, namely to a Kadomtsev–Petviashvili equation. It is shown that dark or antidark soliton stripes, as well as dark lumps, are possible depending on the strength of nonlocality: dark (antidark) solitons are formed for weaker (stronger) nonlocality, relatively to a threshold that is analytically determined in terms of the parameters of the system and the continuous-wave amplitude. Direct numerical simulations are used to show that dark lump-like- and vortex-like-structures can spontaneously be formed as a result of the transverse instability of the dark soliton stripes.

1 Introduction

Natural occurring phenomena are often described by systems exhibiting complicated nonlinear features. It is, therefore, expected that there is much interest in the development of methods to investigate the associated nonlinear mathematical problems. One of the main difficulties in the study of nonlinear phenomena is that the underlying equations are extremely difficult to analyze even numerically. Typical examples are the Navier–Stokes equations or the Euler system [1] in the theory of water waves, and the Maxwell's equations in electromagnetics [2]. As such, one usually employs perturbation methods to asymptotically reduce these systems to nonlinear evolution equations, which are much simpler than the specific problem at hand [3].

Asymptotic multiscale expansion methods have led to a number of such reductions, for example, the Euler system is reduced to the Korteweg–de Vries (KdV) equation for shallow water waves, and to the nonlinear Schrödinger (NLS) equation for deep water. In a similar fashion, Maxwell's equations lead to the NLS equation under the paraxial and quasi-monochromatic approximations in optics [1,2]. These new, simplified, systems not only

[a] e-mail: horikis@uoi.gr (corresponding author)

provide accurate descriptions of the physical situation under which they are derived, but also exhibit remarkable mathematical properties. Indeed, the KdV and NLS equations spawned a completely new field in evolution equations, namely integrable systems and the concept of integrability under the so-called inverse scattering transform (IST) [4].

One very interesting observation [5] in the theory of integrable systems led to the connection between such systems. While these connections are fascinating, linking equations and their properties are a very limited and rather challenging (if even possible) process. As such, asymptotic methods may also be used to reduce several integrable models to other also integrable equations [6]; a characteristic example in this context is the asymptotic reduction in the defocusing NLS to the KdV equation (see also the recent work [7] and references therein).

The IST has in turn proven to be an invaluable tool for the solution of the initial-value problem for integrable nonlinear systems, and, as a byproduct, it also provides exact solutions. However, the class of such integrable systems is rather narrow; most physically relevant systems are non-integrable. Thus, even more interestingly, relevant connections between integrable and nonintegrable models may provide a tool to construct approximate of nonintegrable models in terms of exact solutions of the related integrable ones. This practice has been proven extremely useful in providing important information on the existence, stability and dynamics of solutions in various physical settings, such as nonlinear optics [8] and atomic Bose–Einstein condensates (BECs) [9,10].

A particularly interesting example is the NLS equation featuring a spatially nonlocal nonlinear response. Such nonlocal NLS models arise in a variety of physical contexts, where they describe optical beam dynamics and solitons in plasmas [11], atomic vapors [12], lead glasses with a thermal nonlinearity [13], as well as in media with long-range inter-particle interactions. The latter include nematic liquid crystals that exhibit long-range molecular reorientational interactions [14], as well as dipolar BECs [15]. Notice that a variant of a nonlocal NLS model, namely the Schrödinger–Poisson equation, appears also in cosmology, where it may describe the dynamics of coherent dark matter made up of ultralight axions (see, e.g., the recent review [16] and references therein).

An important issue in the construction of exact or approximate solutions is their stability or lack thereof. Instabilities are physical phenomena that may occur in nonlinear systems and provide a mechanism to observe the manifestation of strongly nonlinear effects. For example, the Benjamin–Feir instability [17] in water waves (alias modulation instability in optics) leads to the generation of a train of localized waves and is believed to be the main mechanism of rogue wave generation [18]. In higher dimensions, instabilities may be proven to be catastrophic leading to wave collapse in the focusing NLS, or to decay into vortical patterns in the defocusing NLS.

Nonlocal nonlinearity plays a key role on the soliton properties and its stability. In particular, in settings with focusing nonlocal nonlinearities, collapse can be arrested in higher-dimensions [19,20]. This results in the formation of stable solitons that were observed in experiments [12,13] and predicted in theory, even in $(3+1)$-dimensions [21]—see, e.g., reviews [20,22] and references therein. On the other hand, if the nonlocal nonlinearity is of defocusing type, dark solitons may exist [23–26] and can exhibit an attractive interaction [23] rather than a repulsive one, as is the situation in the case of a local nonlinearity—see the reviews [8–10] and references therein. Furthermore, dark solitons which are unstable in higher-dimensions due to the onset of transverse (or "snaking") instability [10,27–29] can be stabilized in a setting exhibiting a nonlocal nonlinearity [30].

Motivated by the above, in this work we study a multicomponent nonlocal NLS system in $(2+1)$-dimensions. Notice that although multicomponent NLS systems have been extensively investigated in the literature (see, e.g., the recent review [31] and the book [32]) and corresponding nonlocal problems have been far less studied (see, e.g., Refs. [33–37]). Here, we use a multiscale expansion method to asymptotically reduce the vector NLS model to a scalar Kadomtsev–Petviashvili (KP) equation. This is a completely integrable extension of the KdV equation in two spatial dimensions [38], which is used to describe shallow-water waves, ion-acoustic solitons in plasmas, and other physical systems [1,39–41]. Exact soliton solutions of the KP equation, such as line solitons and lumps, are then used to construct pertinent approximate soliton solutions of the original nonlocal NLS system; this way, we find solutions in the form of dark and antidark line solitons and dark lumps. Specifically, the organization of the presentation, as well as a brief description of our main results and findings is as follows.

In Sect. 2, we present the model, which finds applications in the interaction between two optical beams of different frequencies propagating in nonlocal media, such as nematic liquid crystals [42–44]. The nonlocal NLS system is assumed to exhibit a defocusing nonlinearity, as is the case of azo-dye-doped nematics [25]. First, we present the continuous-wave (cw) solution and discuss its stability, and then we use a multiscale expansion methods to derive an asymptotic reduction in the model at hand, namely a KP equation. It is found that both versions, KP-I and KP-II (see, e.g., Ref. [1]), are possible, and this depends on the degree of nonlocality. In particular, if the nonlocality parameter of the system is larger (smaller) than a characteristic critical value (which is analytically found in terms of the parameters of the system and the cw amplitude)—or, in other words, if nonlocality is relatively strong (weak)—then the KP is of KP-II (KP-I) type.

In Sect. 3, we use the exact soliton solutions of the KP equations and construct approximate solitons of the original nonlocal model. These approximate solutions are found to be of antidark- or dark-soliton-type, for a strong or weak nonlocality (in the sense mentioned above), respectively. We thus find antidark and dark stripe solitons, as well as dark lump solitons. Direct numerical simulations have already confirmed that all the aforementioned solutions do exist and propagate undistorted in the nonlocal medium [45].

In Sect. 4, we study numerically the transverse dynamics of the soliton stripes. Our motivation stems from the fact that the KP-I line solitons are unstable against long-wavelength transverse perturbations (see, e.g., [4,29]) and decay into lumps [46]. We thus investigate, at first, the transverse dynamics of the dark soliton stripes, which also obey an effective KP-I equation. We find that, typically, relatively shallow dark stripes decay into dark lumps, while deeper stripes decay into vortex–antivortex pairs, as well as into transient dark lumps. On the other hand, antidark soliton stripes are not found to be prone to transverse instability, which can be explained by the fact that they obey an effective KP-II equation, whose line solitons are stable [4]. Thus, antidark solitons decay into radiation under the action of the transverse perturbation.

Finally, in Sect. 5 we summarize our findings, present our conclusions, and discuss possibilities for future work.

2 The model and its analytical consideration

2.1 Linear regime

As mentioned above, the nonlocal NLS model under consideration is motivated by the physics of nematic liquid crystals, where it describes the interaction between two polarized, coherent light beams of two different frequencies evolving in a cell filled with a nematic liquid crystal

[44]. In particular, if u and v are the complex electric field envelopes of the two light beams, and θ is the perturbation of the optical director angle from its static value due to the light beams, then the system is described by the following dimensionless equations [44,47]:

$$iu_t + \frac{d_1}{2}\Delta u - 2g_1\theta u = 0, \tag{1a}$$

$$iv_t + \frac{d_2}{2}\Delta v - 2g_2\theta u = 0, \tag{1b}$$

$$\nu\Delta\theta - 2q\theta + 2(g_1|u|^2 + g_2|v|^2) = 0, \tag{1c}$$

where subscripts denote partial derivatives, t plays the role of the propagation distance (assumed to be along the z-direction) and $\Delta \equiv \partial_x^2 + \partial_y^2$ is the transverse Laplacian. Here, the coefficients $d_{1,2}$ and $g_{1,2}$ characterize, respectively, the diffraction and nonlinearity for the two frequencies, with their relative sign in Eqs. (1a) and (1b) determining the nature of the equation: focusing or defocusing, as in the case of the usual scalar or vector NLS model. Notice that although, typically, nematics exhibit a focusing nonlinearity, they can become defocusing upon inclusion of azo-dye doping [25]. Finally, the parameter q is related to the square of the imposed static field which pretilts the nematic dielectric, while the nonlocality parameter ν measures the strength of the response of the nematic liquid crystal in space. In particular, large ν corresponds to a highly nonlocal response, while in the limit of $\nu \to 0$, Eqs. (1) is reduced to the following vector NLS with a local, Kerr-type nonlinearity:

$$iu_t + \frac{d_1}{2}\Delta u - \frac{2g_1}{q}\left(g_1|u|^2 + g_2|v|^2\right)u = 0, \tag{2a}$$

$$iv_t + \frac{d_2}{2}\Delta v - \frac{2g_2}{q}\left(g_1|u|^2 + g_2|v|^2\right)v = 0. \tag{2b}$$

Below, we will focus on the case of defocusing nonlinearity, and we will thus assume that all parameters involved in Eqs. (1) are positive. In addition, as we are interested in dark or antidark soliton solutions, we supplement the system (1) with the following boundary conditions:

$$|u| \to \rho_0, \quad |v| \to \sigma_0, \quad \theta \to \theta_0, \quad \text{as} \quad x, y \to \pm\infty, \tag{3}$$

where ρ_0, σ_0 and θ_0 are real constants.

The steady state solution of Eqs. (1a)–(1c) is composed of the continuous-waves (cw's) for the u- and v-components,

$$u = \rho_0^{1/2}\exp(-2ig_1\theta_0 t), \tag{4}$$

$$v = \sigma_0^{1/2}\exp(-2ig_2\theta_0 t), \tag{5}$$

and the constant function

$$\theta = \theta_0 = \frac{1}{q}(g_1\rho_0 + g_2\sigma_0). \tag{6}$$

The above constitutes the "background" solution, on top of which we will seek soliton solutions below. Considering small perturbations of this solution behaving like $\exp[i(\boldsymbol{k}\cdot\boldsymbol{r}_\perp - \omega t)]$, with $\boldsymbol{r}_\perp = (x,\ y)$, we find that the perturbations' wavevector $\boldsymbol{k} = (k_x,\ k_y)$ and frequency ω obey the dispersion relation:

$$p_1(k)\omega^4 + p_2(k)\omega^2 + p_3(k) = 0, \tag{7}$$

where the polynomials $p_j(k)$ ($j = 1, 2, 3$) are given by:

$$p_1(k) = 16(\nu k^2 + 2q), \tag{8}$$

$$p_2(k) = -4\nu(d_1^2 + d_2^2)k^6 - 8q(d_1^2 + d_2^2)k^4 - 64(d_1 g_1^2 \rho_0 + d_2 g_2^2 \sigma_0)k^2, \tag{9}$$

$$p_3(k) = d_1^2 d_2^2 \nu k^{10} + 2d_1^2 d_2^2 q k^8 + 16 d_1 d_2 (d_2 g_1^2 \rho_0 + d_1 g_2^2 \sigma_0). \tag{10}$$

and $k^2 = k_x^2 + k_y^2$. It is straightforward to find that, in the defocusing case under consideration (i.e., for positive diffraction and nonlinearity coefficients), the dispersion relation (7) has always real roots, i.e., the cw solution is modulationally stable.

2.2 Nonlinear regime: the KP equations

Next, we proceed by analyzing Eqs. (1a)–(1c) by means of a multiscale expansion method. This way, we will derive an effective KP equation, the solutions of which will be exploited for the construction of soliton solutions of the original nonlocal NLS system.

First, we introduce the Madelung transformation for the fields u and v, namely,

$$u = \rho^{1/2} \exp(i\phi), \quad v = \sigma^{1/2} \exp(i\psi), \tag{11}$$

where the real functions $\rho = \rho(\boldsymbol{r}, t)$ and $\sigma = \sigma(\boldsymbol{r}, t)$, as well as $\phi = \phi(\boldsymbol{r}, t)$ and $\psi = \psi(\boldsymbol{r}, t)$, denote amplitudes and phases of the fields u and v, respectively; here, $\boldsymbol{r} = (x, y)$. Then, Eqs. (1) is reduced to the following hydrodynamic form:

$$\rho_t + d_1 \nabla \cdot (\rho \nabla \phi) = 0, \tag{12a}$$

$$\phi_t + 2g_1\theta + \frac{d_1}{2}\left(|\nabla\phi|^2 - \rho^{-1/2}\Delta\rho^{1/2}\right) = 0, \tag{12b}$$

$$\sigma_t + d_2 \nabla \cdot (\sigma \nabla \psi) = 0, \tag{12c}$$

$$\psi_t + 2g_2\theta + \frac{d_2}{2}\left(|\nabla\psi|^2 - \sigma^{-1/2}\Delta\sigma^{1/2}\right) = 0, \tag{12d}$$

$$\nu\Delta\theta - 2q\theta + 2(g_1\rho + g_2\sigma) = 0, \tag{12e}$$

where $\nabla \equiv (\partial_x, \partial_y)$ is the gradient operator. Next, we seek small-amplitude solutions on top of the background solution (4)–(6) in the form of the following asymptotic expansions in ε:

$$\rho = \rho_0 + \varepsilon\rho_1 + \varepsilon^2\rho_2 + \cdots, \tag{13a}$$

$$\phi = -2g_1\theta_0 t + \varepsilon^{1/2}\phi_1 + \varepsilon^{3/2}\phi_2 + \cdots, \tag{13b}$$

$$\sigma = \sigma_0 + \varepsilon\sigma_1 + \varepsilon^2\sigma_2 + \cdots, \tag{13c}$$

$$\psi = -2g_2\theta_0 t + \varepsilon^{1/2}\psi_1 + \varepsilon^{3/2}\psi_2 + \cdots, \tag{13d}$$

$$\theta = \theta_0 + \varepsilon\theta_1 + \varepsilon^2\theta_2 + \cdots, \tag{13e}$$

where the unknown fields ρ_j, ϕ_j, θ_j, σ_j and ψ_j (with $j = 1, 2, \ldots$) depend on the slow variables:

$$X = \varepsilon^{1/2}(x - ct), \quad Y = \varepsilon y, \quad T = \varepsilon^{3/2} t. \tag{14}$$

Here, c is the velocity of linear plane waves propagating on top of the background solution (so-called speed of sound), which will be determined below in a self-consistent manner. Notice that, according to the original boundary conditions (3), the unknown fields must satisfy $\rho_j,\ \phi_j,\ \theta_j,\ \sigma_j,\ \psi_j \to 0$ as $X, Y \to \infty$. Substituting the expansions (13) into Eqs. (1a)–(1c), and using the variables (14) we obtain, at each order of ε, a hierarchy of equations. These equations are consistently solved at each order (see details in "Appendix"), and the following results are obtained.

First, to the leading-order approximation, we obtain the speed of sound, which is given by:

$$c^2 = \frac{2}{q}(d_1 g_1^2 \rho_0 + d_2 g_2^2 \sigma_0), \tag{15}$$

as well as the following equations connecting the fields ρ_1, σ_1, ϕ_1 and ψ_1:

$$\rho_{1X} = \frac{d_1 g_1 \rho_0}{d_2 g_2 \sigma_0} \sigma_{1X}, \tag{16}$$

$$\phi_{1X} = \frac{c}{d_1 \rho_0} \rho_1, \tag{17}$$

$$\psi_{1X} = \frac{c}{d_2 \sigma_0} \sigma_1. \tag{18}$$

Second, to the next order of approximation, we derive the KP equation:

$$(\rho_{1T} + A\rho_{1XXX} + B\rho_1\rho_{1X})_X + \frac{c}{2}\rho_{1YY} = 0, \tag{19}$$

where the coefficients A and B are given by:

$$A = \frac{\nu c^4 - (d_1^3 g_1^2 \rho_0 + d_2^3 g_2^2 \sigma_0)}{4qc^3}, \tag{20a}$$

$$B = \frac{3(g_1^3 d_1^2 \rho_0 + g_2^3 d_2^2 \sigma_0)}{c d_1 g_1 \rho_0 q}. \tag{20b}$$

Importantly, the above analysis ends up with a *single* KP equation for the unknown field ρ_1. Once this function assumes the form of a KP soliton, the unknown field σ_1, as well as the phases ϕ_1 and ψ_1 can be obtained from Eqs. (16)–(18).

We can now further normalize the KP equation (19) in order to express it in its "standard" form [38,40]. We thus introduce the scale transformations:

$$T \mapsto AT, \quad Y \mapsto \sqrt{\frac{6|A|}{c}}Y, \quad \rho_1 \mapsto \frac{B}{6A}\rho_1, \tag{21}$$

and put Eq. (19) into the form:

$$(\rho_{1T} + \rho_{1XXX} + 6\rho_1\rho_{1X})_X + 3\sigma\rho_{1YY} = 0, \quad \sigma \equiv \mathrm{sgn}(A). \tag{22}$$

It is thus clear that the type of KP equation is determined by the value of σ, i.e., the sign of parameter A (notice that B is always positive): For $\sigma = +1$ ($A > 0$), the KP equations are of KP-II type, while for $\sigma = -1$ ($A < 0$) the KP equations are of KP-I type. It is important to point out that σ not only characterizes the equation, but also the type of the soliton themselves: indeed, the solitons may be of bright ($A > 0$) or dark ($A < 0$) type on top of the background solution—see normalization of ρ_1 in Eq. (21). Note that σ depends on the degree of nonlocality—see below.

3 Approximate soliton solutions

We now proceed by constructing approximate [valid up to order $O(\varepsilon)$] soliton solutions of the original nonlocal system (1). This can be expressed in terms of the soliton solutions ρ_1

of the KP equation (19) as follows:

$$u \approx (\rho_0 + \varepsilon\rho_1)^{1/2} \exp\left[-2ig_1\theta_0 t + i\varepsilon^{1/2}\frac{c}{d_1\rho_0}\int \rho_1 \mathrm{d}X\right], \tag{23a}$$

$$\upsilon \approx \left(\sigma_0 + \varepsilon\frac{d_2 g_2\sigma_0}{d_1 g_1\rho_0}\rho_1\right)^{1/2} \exp\left[-2ig_2\theta_0 t + i\varepsilon^{1/2}\frac{cg_2}{d_1 g_1\rho_0}\int \rho_1 \mathrm{d}X\right], \tag{23b}$$

$$\theta \approx \theta_0 + \varepsilon\frac{g_1}{q}\left(1 + \frac{d_2 g_2^2\sigma_0}{d_1 g_1^2\rho_0}\right)\rho_1, \tag{23c}$$

where it is reminded that the background amplitudes ρ_0 and σ_0 are arbitrary $O(1)$ parameters, while θ_0 is given in Eq. (6). Next, we will present certain types of these approximate soliton solutions, which will play an important role in the study of the transverse dynamics below.

3.1 Antidark and dark stripe solitons

We start with the simplest soliton solution of Eq. (19), the so-called line soliton, which is actually a tilted KdV soliton in the xy-plane. The one-line soliton solution of Eq. (19) reads:

$$\rho_1 = \frac{12A}{B}\kappa^2 \mathrm{sech}^2\xi, \tag{24}$$

$$\xi \equiv \kappa\left[X + \lambda\sqrt{\frac{6|A|}{c}}Y - A(4\kappa^2 + 3\lambda^2)T + \delta_0\right], \tag{25}$$

where the free, $O(1)$, parameters κ and λ control the propagation direction in the plane, and δ_0 sets the initial soliton location. Using Eqs. (20), it can readily be found that the soliton amplitude is given by:

$$\frac{12A}{B}\kappa^2 = (\nu - \nu_c)\frac{c^2 d_1 g_1\rho_0}{d_1^3 g_1^2\rho_0 + d_2^3 g_2^2\sigma_0}\kappa^2, \tag{26}$$

where the critical value ν_c is given by:

$$\nu_c = \frac{1}{c^4}(d_1^3 g_1^2\rho_0 + d_2^3 g_2^2\sigma_0). \tag{27}$$

Observe that, since the fraction in the right-hand side of Eq. (26) is always positive, the type of soliton of Eq. (19) depends on the sign of $\nu - \nu_c$, which is:

$$\mathrm{sgn}(\nu - \nu_c) = \mathrm{sgn}(\sigma). \tag{28}$$

This means that both the type of KP equation and the stability of its line soliton solution depend on the degree of nonlocality, and specifically:

- If $\nu > \nu_c$ ($\sigma = +1$), i.e., for a relatively *strong nonlocality*, Eq. (19) is of KP-II type, and its line soliton solution (24) gives rise to *antidark* stripe solitons [see Eqs. (23)], namely intensity elevations on top of the cw background.
- If $\nu < \nu_c$ ($\sigma = -1$), i.e., for a relatively *weak nonlocality* [in other words, closer to the local NLS limit—see Eqs. (2)], Eq. (19) is of KP-I type and its line soliton solution (24) leads to approximate *dark* soliton stripes [see Eqs. (23)], i.e., intensity dips off of the cw background.

Examples of the profiles of the approximate antidark and dark line soliton solutions are given in Figs. 1 and 2, respectively. Regarding the antidark solitons, we have made the

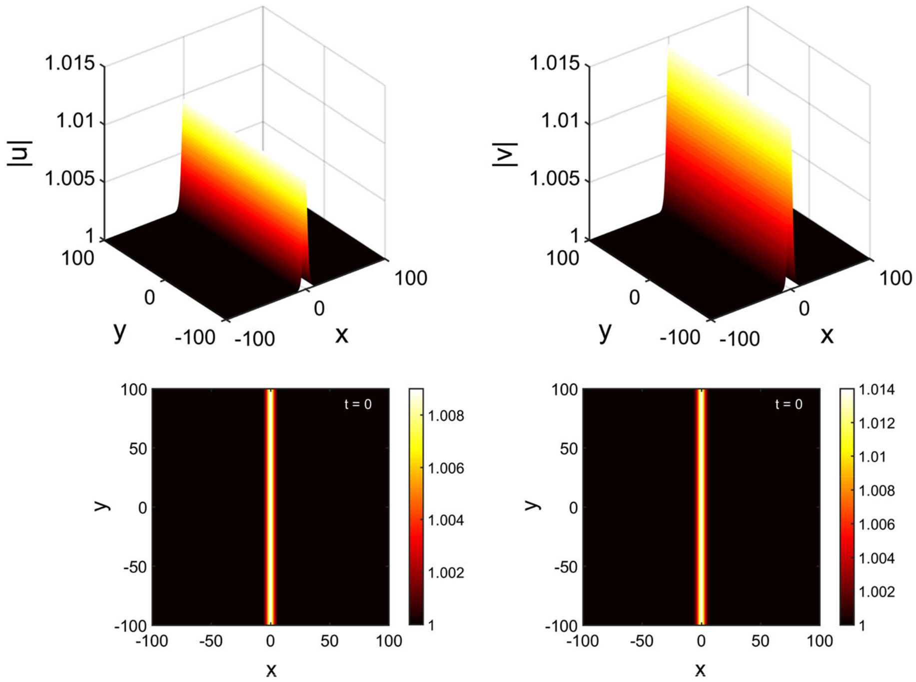

Fig. 1 The spatial profile of the modulus of the antidark stripe solitons at $t = 0$; parameter values are given in the text. Left (right) panels depict the u- (v-)component

following choice for the parameter values: for the NLS system $d_1 = 2d_2/3 = g_1 = g_2 = \nu/5 = q/5 = 1$, for the background amplitudes $\rho_0 = \sigma_0 = 1$, and for the soliton parameters $\lambda = \delta_0 = 0$ and $\kappa = 1$. Note that this choice leads to $A = 1/32 > 0$, $B = 39/20 > 0$, and $\nu_c = 35/8 < \nu$ (i.e., $\sigma = +1$), which means that the solitons are indeed of antidark type and the amplitude function ρ_1 obeys the KP-II equation.

On the other hand, in the case of dark solitons, we used the parameter values $d_1 = 2d_2/3 = g_1 = g_2 = \nu = q/5 = 1$, background amplitudes $\rho_0 = \sigma_0 = 1$, and soliton parameters $\lambda = \delta_0 = 0$, $\kappa = 1$ as before. For this choice, one obtains $A = -27/160 < 0$, $B = 39/20$ and $\nu_c = 35/8 > \nu = 1$ (i.e., $\sigma = -1$), which corresponds to the regime where dark solitons can be formed. Finally, in both cases of antidark and dark solitons, we used $\varepsilon = 0.1$.

3.2 Dark lump solitons

Apart from the 1D stripe soliton solutions that were presented above, the KP-I equation (for $A < 0$, or $\sigma = -1$, corresponding to the weakly nonlocal regime) supports also genuinely 2D solitons. These states, known as "lumps" [38], are weakly localized, i.e., algebraically decaying at infinity. A lump solution of Eq. (19) is of the form:

$$\rho_1(X, Y, T) = \frac{24A}{B} \frac{-\frac{3A}{\alpha} - (X + \alpha T)^2 + \frac{2\alpha Y^2}{c}}{\left(-\frac{3A}{\alpha} + (X + \alpha T)^2 + \frac{2\alpha Y^2}{c}\right)^2}, \tag{29}$$

where α is a $O(1)$ free parameter linking the soliton amplitude with its velocity and transverse width. Notice that, since here $\sigma = -1$, we have $A < 0$, meaning that the vector soliton

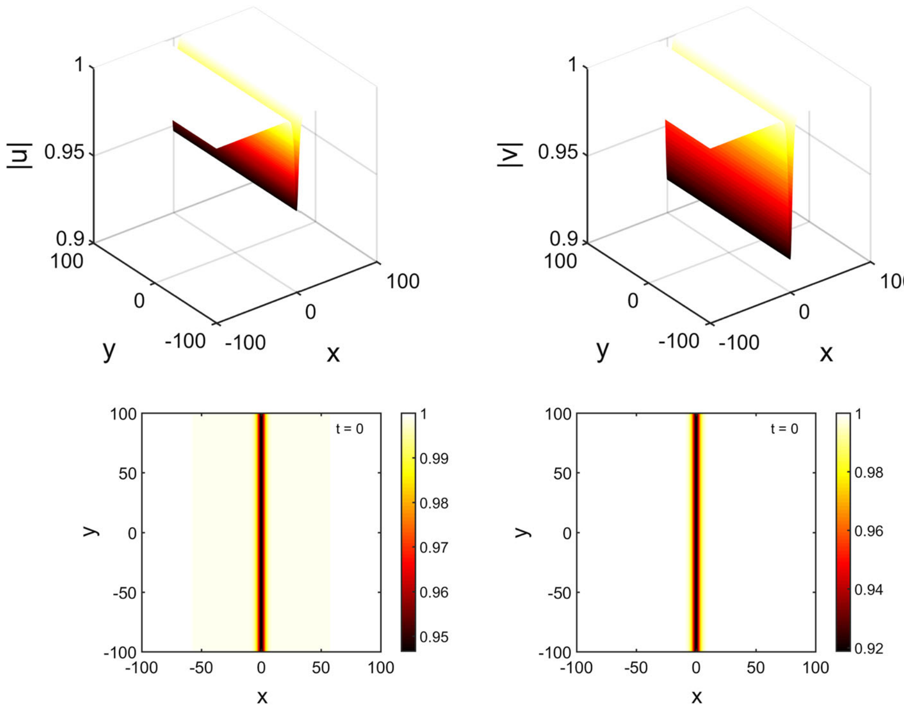

Fig. 2 Similar to Fig. 1, but for the case of dark stripe solitons

solution (23) is of dark type; in other words, in this case, the approximate 2D soliton solutions supported by the nonlocal NLS system are *dark lumps*. An example of this type of solution is shown in Fig. 3; here, we used $\alpha = 1$, while the rest of the parameter values are as in the case of the dark soliton stripe.

Direct numerical simulations have shown [45] that all the above types of approximate soliton solutions do exist and propagate undistorted up to the numerical horizon (i.e., up to $t = 50$). Thus, if no additional perturbations are present, the dark and antidark line solitons and the dark lumps are supported by the nonlocal system. Below, we will numerically study the transverse instability of the line solitons and show, in particular, that sufficiently weak dark line solitons decay into dark lumps under the action of transverse perturbations; this highlights the connection between these solutions, as well as their relation to known results regarding the line solitons of the KP equation.

4 Transverse dynamics

Before proceeding with the numerical investigation of the line solitons' transverse dynamics, it is relevant to make the following comments. As is well known (see, e.g., [4,29] and references therein), the line soliton solutions of KP-II (KP-I) are stable (unstable) under the action of long-wavelength transverse perturbations; in such a situation, the line solitons develop strong undulations and eventually decay—see, e.g., the review [29] for analysis and references therein, as well as Ref. [46] for results of numerical simulations.

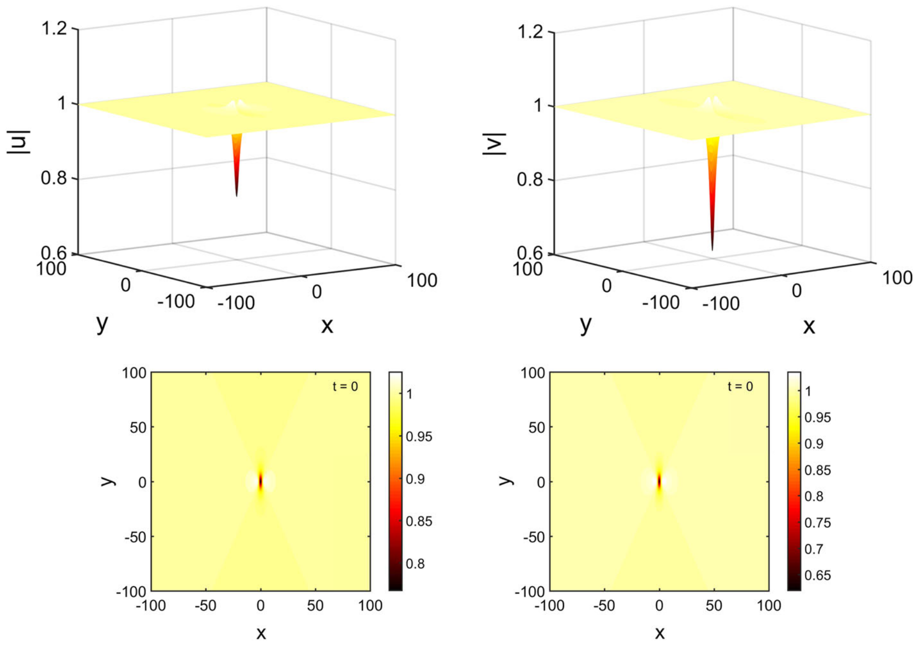

Fig. 3 Similar to Fig. 2, but now for the dark lump soliton, with $\alpha = 1$

In addition, it should be pointed out that the asymptotic reduction in the defocusing 2D NLS (with a local nonlinearity) to the KP-I equation [27,28] was used to better understand the transverse instability of the dark solitons of NLS: indeed, these structures are also subject to transverse instability and, upon developing undulations, they eventually decay into vortex pairs [28,29] or, in the case of shallow dark solitons, into 2D vorticity-free structures resembling KP lumps [28,48]. Furthermore, it was recently shown [30] that nonlocality can partially suppress the transverse instability, in the sense that it manifests itself at later times compared to the local NLS case. It is thus relevant to investigate whether the above features can also be met in the framework of the present model.

To investigate the above, we perform direct numerical simulations by means of a high accuracy spectral method [49], with the following parameter values: $d_1 = d_2 = g_1 = g_2 = q = 1$, and set the nonlocality parameter $\nu = 10$, so as to ensure that we are sufficiently far away from the local limit ($\nu \to 0$). As for the initial condition, we consider a dark stripe soliton pair on top of a background of unit amplitude, located along the y-direction, of the following form:

$$u = \sqrt{1 - w_1^2} \tanh\left(\sqrt{1 - w_1^2} x\right) + i w_1, \tag{30a}$$

$$v = \sqrt{1 - w_2^2} \tanh\left(\sqrt{1 - w_2^2} x\right) + i w_2, \tag{30b}$$

where w_j and $1 - w_j^2$ (with $j = 1, 2$) denote the dark solitons' velocities and amplitudes, respectively. Notice that the above form is motivated by the vector dark soliton of the local NLS; this choice is made in order to highlight the generic nature of our findings. In addition, we assume that w_j are modulated along the transverse (y) direction as follows:

$$w_j = w_j^{(0)}[1 + \delta \cos(\kappa_0 y)], \tag{31}$$

where $w_j^{(0)}$ are the unperturbed values of w_j, the parameter δ is the modulation strength, and κ_0 is the perturbation wavenumber. Below, we use the values $\delta = 0.1$ and $\kappa_0 = 3$.

We start by presenting results pertaining to relatively weak dark stripe solitons, with $w_1^{(0)} = 0.6$ and $w_2^{(0)} = 0.8$. As seen in Fig. 4, where the evolution of the dark stripe soliton pair is shown, the transverse instability manifests itself, and the stripe solitons are eventually destroyed. Although the perturbation induces emission of a relatively strong radiation—compared to the solitons' amplitudes—which propagates on top of the background, it is clear that a chain of 2D structures is formed in both components: see the snapshots corresponding to $t = 50$ and $t = 100$.

A zoom of a pair of the 2D states, at $t = 100$, that are generated due to the manifestation of the instability, is presented in Fig. 5; there, both the moduli and the phases of the fields u and v are shown. Despite the radiation-induced perturbation, it is clearly observed that the generated structures are vorticity-free states (see the phase profiles in the bottom panels), resembling the dark lump solitons discussed above.

Let us now proceed by investigating the case of relatively deep dark soliton stripes. For this case, we again consider the initial conditions (30) and use $w_1^{(0)} = 0.3$ and $w_2^{(0)} = 0.4$. The results of the relevant simulations are shown in Fig. 6. Once again, it is observed that the transverse instability causes the stripes to undergo strong modulations and, as a result, they are eventually destroyed. In this case, the radiation on the background is relatively smaller compared to the solitons' amplitudes, and the resulting patterns that are formed out of the instability can easier be identified.

In particular, first we note that the destruction of the dark stripes results in the formation of a chain of pairs of 2D structures, located close to $x = 30$, that are clearly visible in both components at $t = 75$. Figure 7 shows a zoom-in of Fig. 6, where the moduli profiles (top panels) and the relevant phases (bottom panels) of the fields u and v are depicted. Clearly, the structure of these profiles corresponds to vortex–antivortex pairs—see, e.g., Ref. [31]. This clearly highlights the fact that the transverse instability of relatively deep dark soliton stripes of the nonlocal NLS leads to the formation of vortex pairs, similarly to the case of the local NLS (see, e.g., the review [29]).

In addition to the array of vortex antivortex pairs, the formation of another chain of 2D structures is also observed. Such chains are seen, e.g., close to $x = 55$ at $t = 75$ in the v-component, or close to $x = 80$ at $t = 100$ in the v-component. Contrary to the case of the vortex arrays that show a slow motion, the chains of 2D density dips continue to travel in the x direction, and form a propagating front modulated along the y direction. A zoom of these structures in the v-component, close to $x = 55$ for $t = 75$, is shown in Fig. 8. It is observed that both the modulus and phase of these density dips resemble those of the dark lump solitons. Thus, even in the case of relatively deep dark stripes, the transverse instability leads to the formation of transient dark lump solitons.

We finally mention that we have also performed relevant simulations with transversely perturbed antidark soliton stripes, using the initial condition for u:

$$u = \sqrt{1 - w^2}\,\mathrm{sech}(\sqrt{1 - w^2}x) + iw, \tag{32}$$

and a similar form for v, as in the case of dark stripe solitons. Once again, w is taken in the form of Eq. (31), while the considered parameter values are the same as before. As one should expect from the fact that these states are governed by an effective KP-II equation,

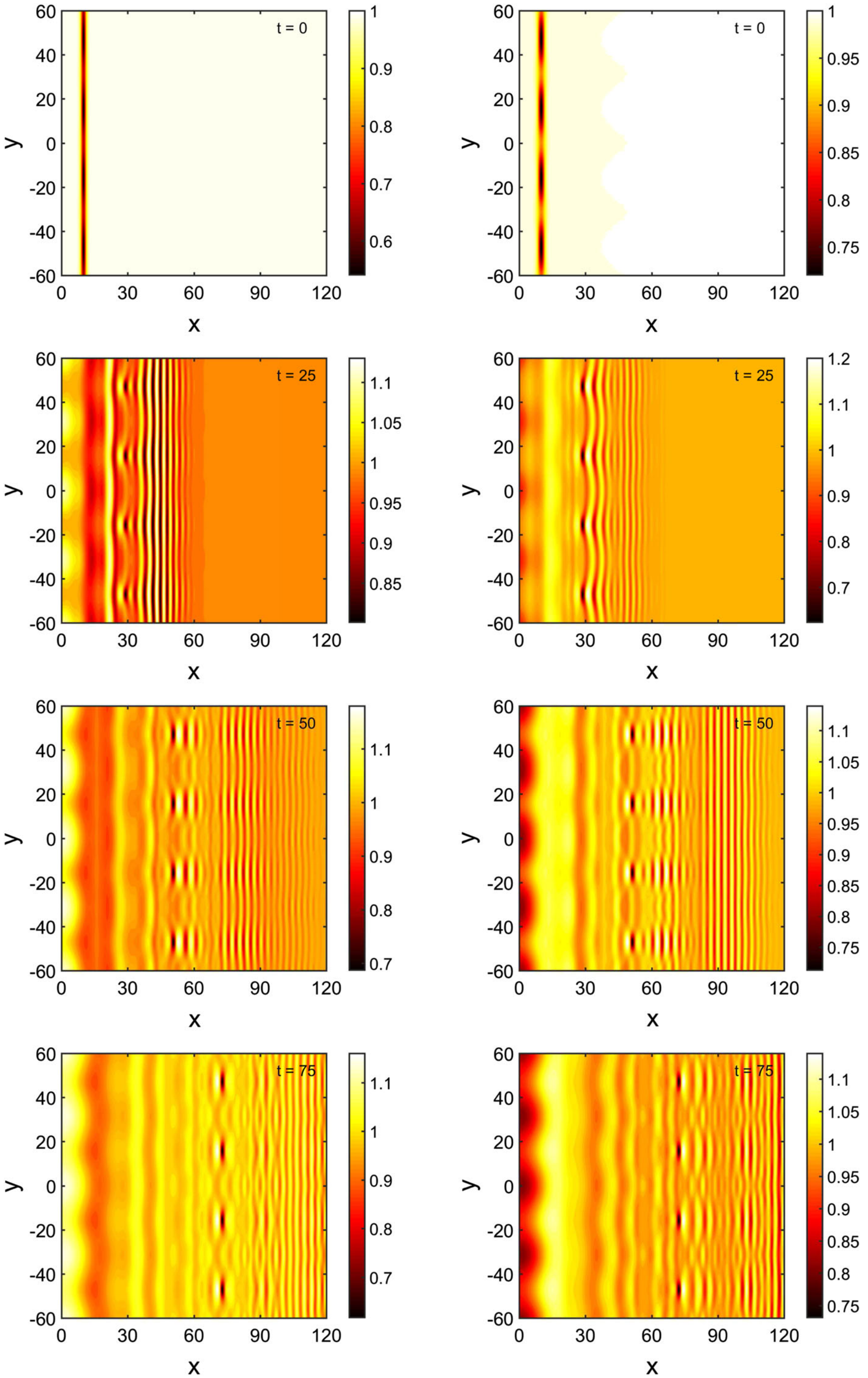

Fig. 4 Contour plots showing the evolution of perturbed, relatively shallow dark soliton stripes, with $w_1^{(0)} = 0.6$ and $w_2^{(0)} = 0.8$ (see text). From top to bottom, left (right) panels depict the modulus of the field u (v) at $t = 0, 25, 50$, and 75. The dark solitons in both components decay into 2D structures resembling KP-I lumps

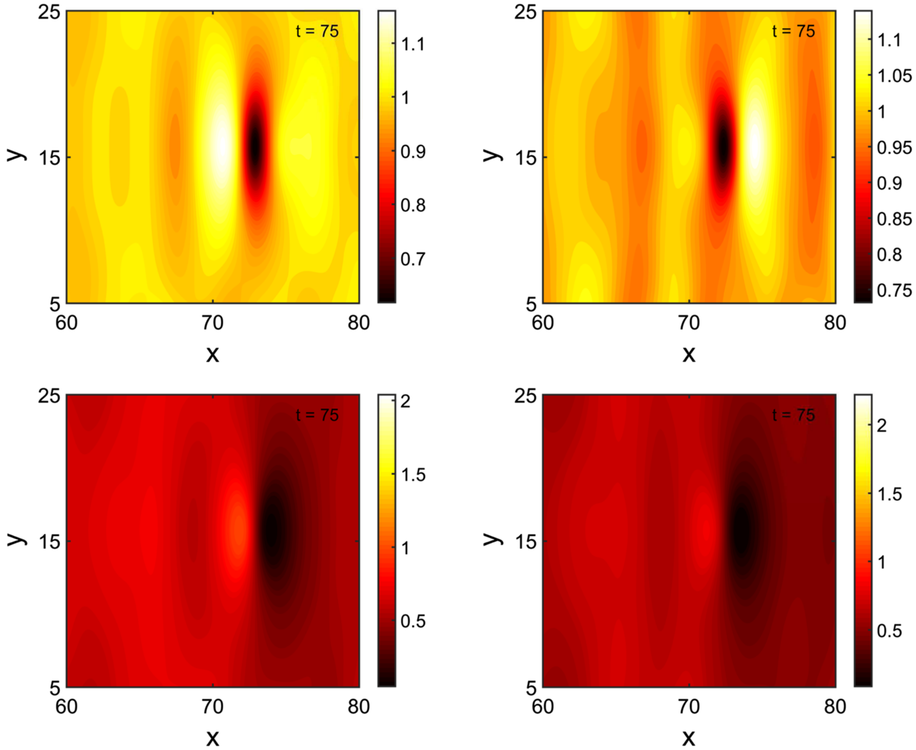

Fig. 5 A zoom of Fig. 4 depicting the modulus (top panels) and phase (bottom panels) of the fields u (left panels) and v (right panels), at $t = 75$. Despite the radiation-induced perturbation, it is observed that the emerged 2D waveforms are vorticity-free structures resembling KP-I lumps

we found that these solitons are not prone to transverse instability. In particular, as seen in Fig. 9, the perturbation destroys the antidark stripes, which eventually decay into radiation. Contrary to the case of dark solitons, here the instability of the antidark stripes does not give rise to the formation of 2D structures.

5 Conclusions and discussion

In this work, we studied the formation and dynamics of vector solitons in media with a spatially nonlocal nonlinear response. The considered model, namely a two-component nonlocal nonlinear Schrödinger (NLS) equation featuring a defocusing nonlinearity, finds applications in the interaction of two optical beams of different frequencies, which propagate in an azo-dye-doped nematic liquid crystal. We considered solutions that propagate on top of a continuous-wave solution in both components, and we employed a multiscale expansion method to asymptotically reduce the original vector model to a completely integrable scalar one, namely to the well-known Kadomtsev–Petviashvili (KP) equation. This way, line and lump KP solitons were used for the construction of approximate stripe soliton and lump solitons on the cw background.

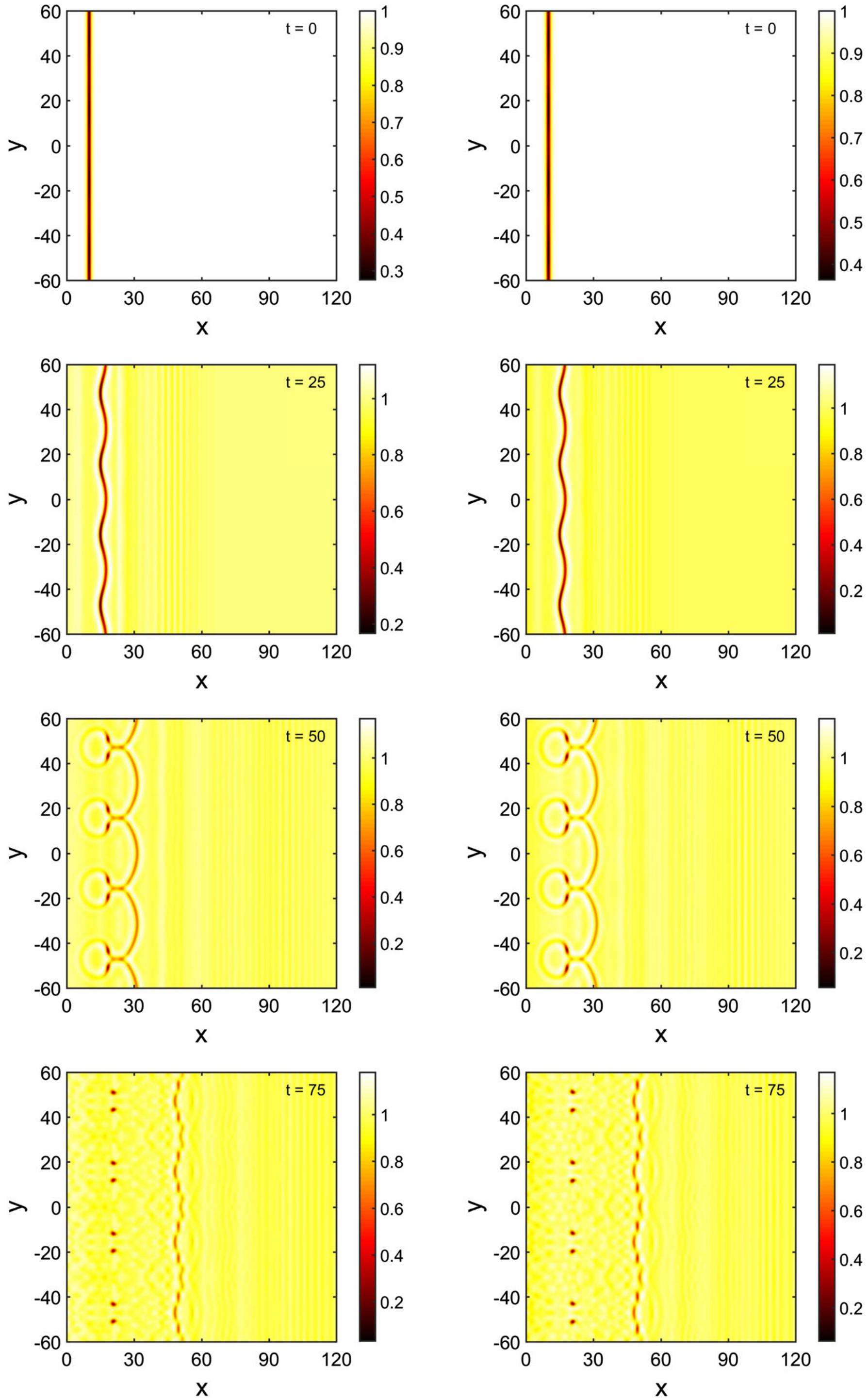

Fig. 6 Similar to Fig. 4, but now for relatively deep dark soliton stripes, with $w_1^{(0)} = 0.3$ and $w_2^{(0)} = 0.4$

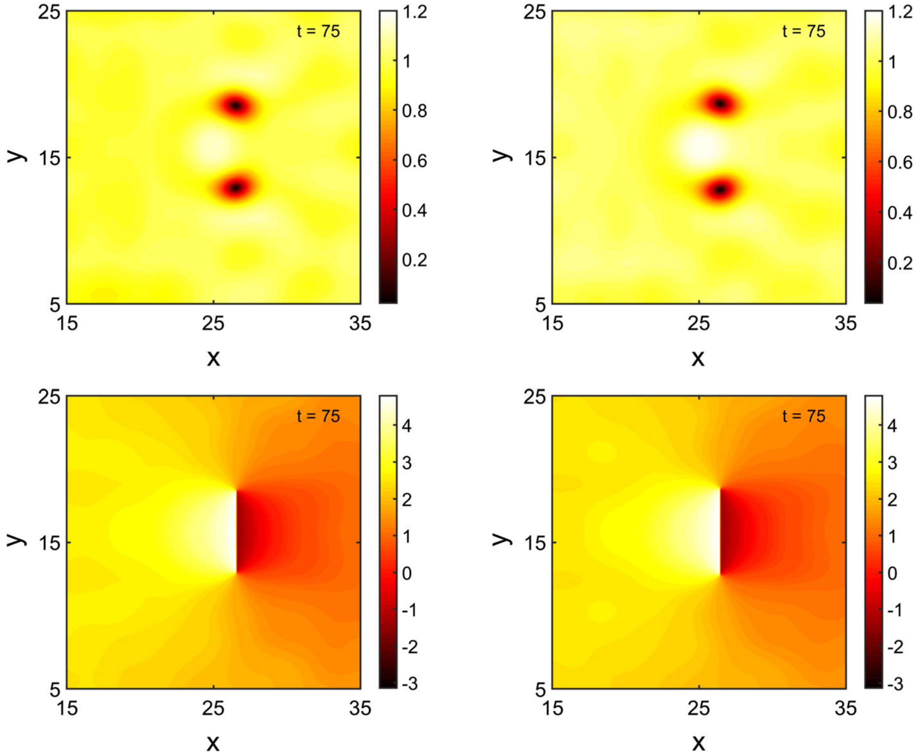

Fig. 7 A zoom of Fig. 6 depicting the modulus (top panels) and phase (bottom panels) of the fields u (left panels) and v (right panels), at $t = 75$. It is observed that the 2D waveforms in both components are vortex–antivortex pairs

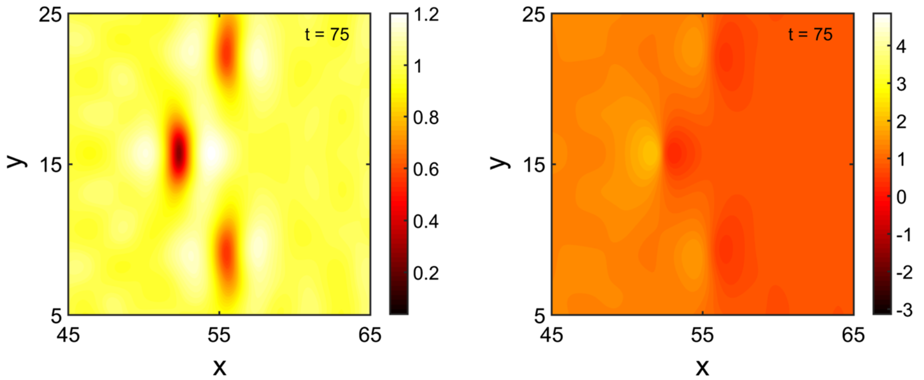

Fig. 8 A zoom of Fig. 6 showing the modulus (left panel) and phase (right panel) of 2D structures, located close to $x = 55$, that are formed in the field v at $t = 75$. These structures are density dips resembling KP-I lumps

Our analysis revealed that the version of the KP equation (KP-I or KP-II), as well as the type of solitons (dark or antidark) on the background, is determined by the degree of nonlocality of the original system. In particular, we found that if ν is the parameter characterizing the

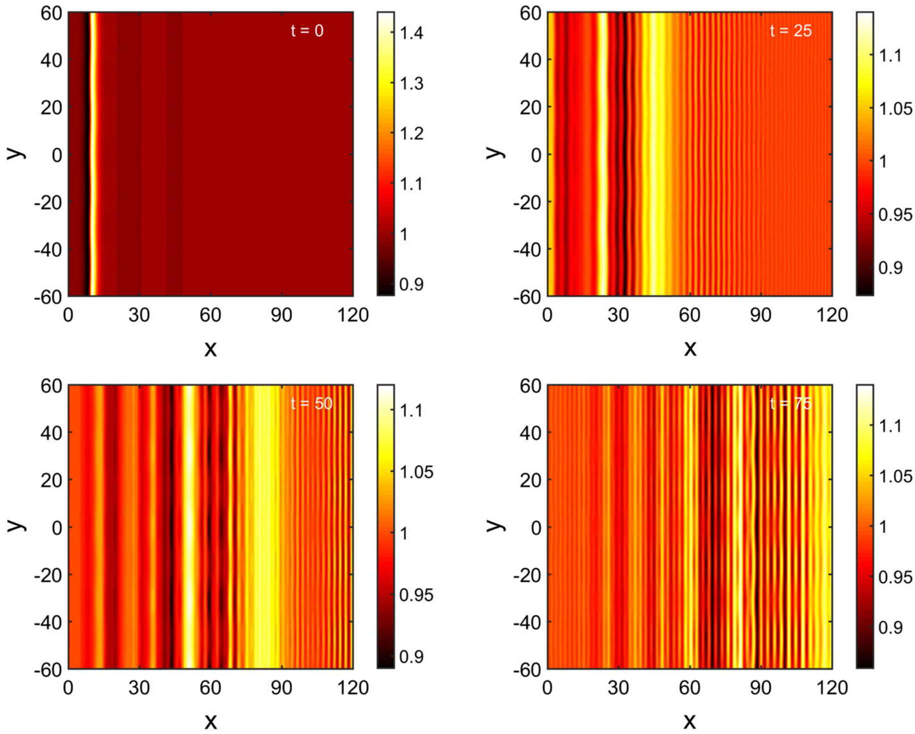

Fig. 9 Contour plots depicting the evolution of the modulus of the field u, carrying a perturbed antidark soliton; shown are snapshots at $t = 0$ [initial condition—see Eq. (32)], $t = 25$, $t = 50$, and $t = 75$

degree of nonlocality, then there exists a critical value ν_c (depending on the parameters of the system and the background amplitudes) such that: if $\nu > \nu_c$, then the KP equation is of KP-II type, and the solitons are antidark; on the other hand, if $\nu < \nu_c$ (i.e., when nonlocality is weak and we are thus closer to the local NLS limit), then the KP equation is of KP-I type, and the solitons are dark. The change of character of the KP equation below or above the nonlocality threshold is reminiscent of a similar situation in the shallow water wave problem: if surface tension is weak, then the KP is of KP-II type, while if it is strong (in the sense that it dominates gravity), then the KP is of KP-I type. This suggests that the degree of nonlocality plays the role of an *analog of surface tension*, similarly to the case of the pertinent single-component nonlocal NLS model [50].

Our analytical approach shows that the soliton amplitudes in the u- and v-components are connected to each other and thus they are governed by a single KP equation. The soliton states that were predicted to occur are: antidark and dark soliton stripes (corresponding to the stable and unstable line solitons of KP-II and KP-I, respectively), as well as dark lump solitons (pertinent to KP-I). In addition, we performed numerical simulations to study the transverse dynamics of the stripe solitons. This investigation was motivated by the following question: are dark (or antidark) soliton stripes of the nonlocal NLS prone to the transverse instability, given that they obey an effective KP-I (or KP-II) equation, where line solitons are unstable (stable)? Our simulations revealed that, indeed, relatively shallow dark stripe solitons decay into dark lumps, which correspond to the stable 2D soliton solutions of the KP-I equation. In addition, relatively deep dark stripes were found to decay into a chain of vortex–antivortex pairs, as well as into a transient array of dark lump solitons. Thus, we can safely conclude that dark lumps, as well as vortex–states can spontaneously be formed as a result of the transverse ("snaking") instability of dark soliton stripes in nonlocal media. On the other hand, we have found that antidark solitons that are governed by an effective KP-II equation are not prone to snaking: indeed, under transverse perturbation, they decay into radiation, without giving rise to the emergence of 2D structures.

Our analysis and results pave the way for other interesting future research themes. For instance, it would be interesting to investigate if other, quasi-one-dimensional states having, e.g., the form of dark-bright soliton stripes, or ring solitons of the dark or the antidark type, as well as purely 2D structures, such as vector vortices or vortex-bright solitons [51] can be supported in multi-component nonlocal media. Such investigations are currently in progress, and relevant results will be reported elsewhere.

Appendix: Derivation of the KP equation

Here, we provide details on the perturbation expansion and the derivation of the KP equation. First, Eq. (12a) yields:

$$O(\varepsilon^{3/2}): \quad -c\rho_{1X} + d_1\rho_0\phi_{1XX} = 0, \tag{33}$$

$$O(\varepsilon^{5/2}): \quad \rho_{1T} - c\rho_{2X} + d_1\left[(\rho_1\phi_{1X})_X + \rho_0\phi_{1YY} + \rho_0\phi_{2XX}\right] = 0. \tag{34}$$

From Eq. (12b), we obtain:

$$O(\varepsilon): \quad -c\phi_{1X} + 2g_1\theta_1 = 0, \tag{35}$$

$$O(\varepsilon^2): \quad \phi_{1T} - c\phi_{2X} + 2g_1\theta_2 + \frac{d_1}{2}\left(\phi_{1X}^2 - \frac{1}{2\rho_0}\rho_{1XX}\right) = 0. \tag{36}$$

Equation (12c) yields:

$$O(\varepsilon^{3/2}): \quad -c\sigma_{1X} + d_2\sigma_0\psi_{1XX} = 0, \tag{37}$$

$$O(\varepsilon^{5/2}): \quad \sigma_{1T} - c\sigma_{2X} + d_2\left[(\sigma_1\psi_{1X})_X + \sigma_0\phi_{1YY} + \sigma_0\psi_{2XX}\right] = 0. \tag{38}$$

From Eq. (12d), we obtain:

$$O(\varepsilon): \quad -c\psi_{1X} + 2g_2\theta_1 = 0, \tag{39}$$

$$O(\varepsilon^2): \quad \psi_{1T} - c\psi_{2X} + 2g_2\theta_2 + \frac{d_2}{2}\left(\psi_{1X}^2 - \frac{1}{2\sigma_0}\sigma_{1XX}\right) = 0, \tag{40}$$

and, finally, Eq. (12e) leads to:

$$O(\varepsilon): \quad -q\theta_1 + g_1\rho_1 + g_2\sigma_1 = 0, \tag{41}$$

$$O(\varepsilon^2): \quad \nu\theta_{1XX} - 2q\theta_2 + 2(g_1\rho_2 + g_2\sigma_2) = 0. \tag{42}$$

We consider the linear equations (33), (35), (37), (39) and (41). This system can be simplified as follows: differentiate Eqs. (35) and (39) with respect to X, and substitute θ_1 from Eq. (41), ϕ_{1XX} from Eq. (33) and ψ_{1XX} from Eq. (37). This yields the following two equations:

$$\left(-\frac{c^2}{d_1\rho_0} + \frac{2g_1^2}{q}\right)\rho_{1X} + \frac{2g_1g_2}{q}\sigma_{1X} = 0, \tag{43}$$

$$\frac{2g_1g_2}{q}\rho_{1X} + \left(-\frac{c^2}{d_2\sigma_0} + \frac{2g_2^2}{q}\right)\sigma_{1X} = 0. \tag{44}$$

The above system for the unknown functions ρ_{1X} and σ_{1X} has nontrivial solutions as long as the determinant of the coefficients is equal to zero. This requirement leads to the speed of sound, given in Eq. (15).

Next, we proceed with the equations at the next order of approximation, namely with Eqs. (34), (36), (38), (40) and (42). First, multiply (36) by $\frac{d_1\rho_0}{c}$ and (40) by $\frac{d_2\sigma_0}{c}$, respectively, and differentiate them with respect to X. Then, adding the resulting equations with (34) and (38), respectively, we obtain the following system of equations:

$$\begin{aligned}
&-c\rho_{2X} + \rho_{1T} + d_1(\rho_1\phi_{1X})_X + d_1\rho_0\phi_{1YY} + \frac{d_1\rho_0}{c}\phi_{1TX} + \frac{2d_1g_1\rho_0}{c}\theta_{2X}\\
&\quad + \frac{d_1^2\rho_0}{2c}(\phi_{1X})_X^2 - \frac{d_1^2}{4c}\rho_{1XXX} = 0,
\end{aligned} \tag{45}$$

$$\begin{aligned}
&-c\sigma_{2X} + \sigma_{1T} + d_2(\sigma_1\psi_{1X})_X + d_2\sigma_0\psi_{1YY} + \frac{d_2\sigma_0}{c}\psi_{1TX} + \frac{2d_2g_2\sigma_0}{c}\theta_{2X}\\
&\quad + \frac{d_2^2\sigma_0}{2c}(\psi_{1X})_X^2 - \frac{d_2^2}{4c}\sigma_{1XXX} = 0,
\end{aligned} \tag{46}$$

$$\nu\theta_{1XX} - 2q\theta_2 + 2(g_1\rho_2 + g_2\sigma_2) = 0. \tag{47}$$

This system can be further simplified as follows. Multiply Eqs. (45) and (46) by $-\frac{g_1}{qc}$ and $-\frac{g_2}{qc}$, respectively, and add the resulting equations. Then, substituting θ_2 from Eq. (47), and using Eqs. (33), (37) and (43), we derive the KP equation (19).

References

1. M.J. Ablowitz, *Nonlinear Dispersive Waves: Asymptotic Analysis and Solitons* (Cambridge University Press, Cambridge, 2011)
2. Y.S. Kivshar, G.P. Agrawal, *Optical Solitons: From Fibers to Photonic Crystals* (Academic Press, London, 2003)
3. A. Jeffrey, T. Kawahara, *Asymptotic Methods in Nonlinear Wave Theory* (Pitman, London, 1982)
4. M.J. Ablowitz, H. Segur, *Solitons and the Inverse Scattering Transform* (SIAM, Philadelphia, 1981)
5. R.M. Miura, Korteweg–de Vries equation and generalizations. I. A remarkable explicit non-linear transformation. J. Math. Phys. **9**, 1202–1204 (1968)
6. V.E. Zakharov, E.A. Kuznetsov, Multi-scale expansions in the theory of systems integrable by the inverse scattering transform. Physica D **18**, 455–463 (1986)
7. T.P. Horikis, D.J. Frantzeskakis, On the NLS to KdV connection. Rom. J. Phys. **59**, 195–203 (2014)
8. YuS Kivshar, B. Luther-Davies, Dark optical solitons: physics and applications. Phys. Rep. **298**, 81–197 (1998)
9. D.J. Frantzeskakis, Dark solitons in Bose–Einstein condensates: from theory to experiments. J. Phys. A Math. Theor. **43**, 213001 (2010)
10. P.G. Kevrekidis, D.J. Frantzeskakis, R. Carretero-González, *The Defocusing Nonlinear Schrödinger Equation: From Dark Solitons to Vortices and Vortex Rings* (SIAM, Philadelphia, 2015)
11. A.G. Litvak, V.A. Mironov, G.M. Fraiman, A.D. Yunakovskii, Thermal self-effect of wave beams in a plasma with a nonlocal nonlinearity. Sov. J. Plasma Phys. **1**, 60–71 (1975)
12. D. Suter, T. Blasberg, Stabilization of transverse solitary waves by a nonlocal response of the nonlinear medium. Phys. Rev. A **48**, 4583–4587 (1993)
13. C. Rotschild, T. Carmon, O. Cohen, O. Manela, M. Segev, Solitons in nonlinear media with an infinite range of nonlocality: first observation of coherent elliptic solitons and of vortex-ring solitons. Phys. Rev. Lett. **95**, 213904 (2005)
14. C. Conti, M. Peccianti, G. Assanto, Route to nonlocality and observation of accessible solitons. Phys. Rev. Lett. **91**, 073901 (2003)

15. P. Pedri, L. Santos, Two-dimensional bright solitons in dipolar Bose–Einstein condensates. Phys. Rev. Lett. **95**, 200404 (2005)
16. L. Arturo Urena-López, Brief review on scalar field dark matter models. Front. Astron. Space Sci. **6**, 47 (2019)
17. T.B. Benjamin, J.E. Feir, The disintegration of wave trains on deep water. Part 1. Theory. J. Fluid Mech. **27**, 417–430 (1967)
18. M. Onorato, S. Residoric, U. Bortolozzo, A. Montina, F.T. Arecchi, Rogue waves and their generating mechanisms in different physical contexts. Phys. Rep. **528**, 47–89 (2013)
19. S.K. Turitsyn, Spatial dispersion of nonlinearity and stability of many dimensional solitons. Theor. Math. Phys. **64**, 797–801 (1985)
20. W. Krolikowski, O. Bang, N.I. Nikolov, D. Neshev, J. Wyller, J.J. Rasmussen, D. Edmundson, Modulational instability, solitons and beam propagation in spatially nonlocal nonlinear media. J. Opt. B Quantum Semiclass. Opt. **6**, S288–S294 (2004)
21. D. Mihalache, D. Mazilu, F. Lederer, B.A. Malomed, Y.V. Kartashov, L.-C. Crasovan, L. Torner, Three-dimensional spatiotemporal optical solitons in nonlocal nonlinear media. Phys. Rev. E **73**, 025601(R) (2006)
22. D. Mihalache, Multidimensional solitons and vortices in nonlocal noninear optical media. Rom. Rep. Phys. **59**, 515–522 (2007)
23. A. Dreischuh, D.N. Neshev, D.E. Petersen, O. Bang, W. Krolikowski, Observation of attraction between dark solitons. Phys. Rev. Lett. **96**, 043901 (2006)
24. Y.V. Kartashov, L. Torner, Gray spatial solitons in nonlocal nonlinear media. Opt. Lett. **32**, 946–948 (2007)
25. A. Piccardi, A. Alberucci, N. Tabiryan, G. Assanto, Dark nematicons. Opt. Lett. **36**, 1356–1358 (2011)
26. T.P. Horikis, Small-amplitude defocusing nematicons. J. Phys. A Math. Theor. **48**, 02FT01 (2015)
27. E.A. Kuznetsov, S.K. Turitsyn, Instability and collapse of solitons in media with a defocusing nonlinearity. JETP **67**, 1583–1588 (1988)
28. D.E. Pelinovsky, YuA Stepanyants, YuS Kivshar, Self-focusing of plane dark solitons in nonlinear defocusing media. Phys. Rev. E **51**, 5016–5026 (1995)
29. YuS Kivshar, D.E. Pelinovsky, Self-focusing and transverse instabilities of solitary waves. Phys. Rep. **331**, 117–195 (2000)
30. A. Armaroli, S. Trillo, Suppression of transverse instabilities of dark solitons and their dispersive shock waves. Phys. Rev. A **80**, 053803 (2009)
31. P.G. Kevrekidis, D.J. Frantzeskakis, Solitons in coupled nonlinear Schrödinger models: a survey of recent developments. Rev. Phys. **1**, 140–153 (2016)
32. M.J. Ablowitz, B. Prinari, A.D. Trubatch, *Discrete and Continuous Nonlinear Schrödinger Systems* (Cambridge University Press, Cambridge, 2004)
33. G. Assanto, N.F. Smyth, A.L. Worthy, Two-color, nonlocal vector solitary waves with angular momentum in nematic liquid crystals. Phys. Rev. A **78**, 013832 (2008)
34. Z. Xu, N.F. Smyth, A.A. Minzoni, YuS Kivshar, Vector vortex solitons in nematic liquid crystals. Opt. Lett. **34**, 1414–1416 (2009)
35. Y. Lin, R.-K. Lee, Dark-bright soliton pairs in nonlocal nonlinear media. Opt. Express **15**, 8781 (2007)
36. W. Chen, Q. Kong, M. Shen, Q. Wang, J. Shi, Polarized vector dark solitons in nonlocal Kerr-type self-defocusing media. Phys. Rev. A **87**, 013809 (2013)
37. T.P. Horikis, D.J. Frantzeskakis, Vector nematicons: coupled spatial solitons in nematic liquid crystals. Phys. Rev. A **94**, 053805 (2016)
38. M.J. Ablowitz, P.A. Clarkson, *Solitons, Nonlinear Evolution Equations and Inverse Scattering* (Cambridge University Press, Cambridge, 1991)
39. V.I. Karpman, *Non-linear Waves in Dispersive Media* (Elsevier Science & Technology, Amsterdam, 1974)
40. E. Infeld, G. Rowlands, *Nonlinear Waves, Solitons and Chaos* (Cambridge University Press, Cambridge, 1990)
41. R.S. Johnson, *A Modern Introduction to the Mathematical Theory of Water Waves* (Cambridge University Press, Cambridge, 1997)
42. G. Assanto, *Nematicons: Spatial Optical Solitons in Nematic Liquid Crystals* (Wiley-Blackwell, New Jersey, 2012)
43. G. Assanto, A.A. Minzoni, N.F. Smyth, Light self-localization in nematic liquid crystals: modelling solitons in nonlocal reorientational media. J. Nonlinear Opt. Phys. Mater. **18**, 657–691 (2009)
44. A. Alberucci, M. Peccianti, G. Assanto, A. Dyadyusha, M. Kaczmarek, Two-color vector solitons in nonlocal media. Phys. Rev. Lett. **97**, 153903 (2006)

45. G.N. Koutsokostas, T.P. Horikis, D.J. Frantzeskakis, B. Prinari, G. Biondini, Multiscale expansions and vector solitons of a two-dimensional nonlocal nonlinear Schrödinger system. Stud. Appl. Math. (2020) (under review)
46. E. Infeld, A. Senatorski, A.A. Skorupski, Decay of Kadomtsev–Petviashvili solitons. Phys. Rev. Lett. **72**, 1345–1347 (1994)
47. B.D. Skuse, N.F. Smyth, Interaction of two-color solitary waves in a liquid crystal in the nonlocal regime. Phys. Rev. A **79**, 063806 (2009)
48. V.A. Mironov, A.I. Smirnov, L.A. Smirnov, Dynamics of vortex structure formation during the evolution of modulation instability of dark solitons. J. Exp. Theor. Phys. **112**, 46–59 (2011)
49. A. Kassam, L.N. Trefethen, Fourth-order time stepping for stiff PDEs. SIAM J. Sci. Comput. **26**, 1214–1233 (2005)
50. T.P. Horikis, D.J. Frantzeskakis, Light meets water in nonlocal media: surface tension in optics. Phys. Rev. Lett. **118**, 243903 (2017)
51. K.J.H. Law, P.G. Kevrekidis, L.S. Tuckerman, Stable vortex-bright-soliton structures in two-component Bose–Einstein condensates. Phys. Rev. Lett. **105**, 160405 (2010)